



Ecballium elaterium improved stimulatory effects of tissue-resident NK cells and ameliorated liver fibrosis in a thioacetamide mice model

Mustafa Ghanim^{a,*}, Johnny Amer^{b,*}, Ahmad Salhab^{a,1}, Nidal Jaradat^c

^a Department of Biomedical Sciences, Faculty of Medicine and Health Sciences, An-Najah National University, P.O. Box 7, Nablus, Palestine

^b Department of Allied and Applied Medical Sciences, Division of Anatomy Biochemistry and Genetics, An-Najah National University, P.O. Box 7, Nablus, Palestine

^c Department of Pharmacy, Faculty of Medicine and Health Sciences, An-Najah National University, P.O. Box 7, Nablus, Palestine

ARTICLE INFO

Keywords:

Ecballium elaterium
Chronic liver injury
Antioxidant markers
TrNK cells

ABSTRACT

Ecballium elaterium (EE), widely used plant in Mediterranean medicine, showed anticancer activity. This study aimed to investigate EE effects on liver fibrosis in an animal model of thioacetamide (TAA). Intraperitoneal administration of TAA was performed twice weekly for four weeks in C57BL6J mice. Livers were extracted and serum were evaluated for inflammatory markers (H&E staining, ALT, AST, ALP), pro-inflammatory cytokines, fibrosis (Sirius red staining, Masson's trichrome, α -smooth muscle actin and collagen III), and metabolic (cholesterol, triglyceride, C-peptide, and fasting-blood-sugar) profiles. Glutathione, glutathione peroxidase, and catalase liver antioxidant markers were assessed. Tissue-resident NK cells from mice livers were functionally assessed for activating receptors and cytotoxicity. Compared to vehicle-treated mice, the TAA-induced liver injury showed attenuation in the histopathology outcome following EE treatment. In addition, EE-treated mice resulted in decreased serum levels of ALT, AST, and ALP, associated with a decrease in IL-20, TGF- β , IL-17, IL-22 and MCP-1 concentrations. Moreover, EE-treated mice exhibited improved lipid profile of cholesterol, triglycerides, C-peptide, and FBS. EE treatment maintained GSH, GPX, and CAT liver antioxidant activity and led to elevated counts of tissue-resident NK (trNK) cells in the TAA-mice. Consequently, trNK demonstrated an increase in CD107a and IFN- γ with improved potentials to kill activated hepatic-stellate cells in an in vitro assay. EE exhibited antifibrotic and antioxidative effects, increased the number of trNK cells, and improved metabolic outcomes. This plant extract could be a targeted therapy for patients with advanced liver injury.

1. Introduction

Liver fibrosis is the abnormal accumulation of the liver's parenchymal cells replaced by fibrous connective tissue. Advanced liver fibrosis can progress to cirrhosis and hepatocellular cancer [1,2]. Several etiologies, including excessive alcohol consumption, drugs, environmental pollutants, chemical toxins, viral infections, and immunological damage, produce liver injury [3]. Liver fibrosis is characterized by the accumulation of collagen and extracellular matrix, leading to distortion of the normal liver architecture, hepatocellular carcinoma, and eventually liver failure, all associated with high morbidity and mortality. Currently, therapies for liver fibrosis are aimed at either managing the primary disease or treating it by consistently lowering

inflammation, preventing oxidative stress, and increasing collagen breakdown [4–7]. However, no effective anti-liver fibrosis medication devoid of apparent adverse effects has been developed. In recent years, several medicinal plants have demonstrated significant benefits in treating many forms of liver illnesses, providing an important source for developing anti-liver fibrosis medications owing to their broad bioactivity and low toxicity. Inflammatory factors and reactive oxygen species have been shown in several studies to play essential roles in the development of liver fibrosis [8]. Therefore, if herbal medicine can enhance the antioxidant defense system, they may produce protective and therapeutic effects against liver fibrosis. *Ecballium elaterium* (EE), which belongs to the family Cucurbitaceae, has been used traditionally in herbal medicine to treat fever, sinusitis, hypertension, rheumatic

Abbreviations: α SMA, α smooth muscle actin; EE, *Ecballium elaterium*; TAA, thioacetamide; trNK, tissue-resident NK; pHSCs, Primary Hepatic Stellate Cells; CD107a, Lysosomal-associated membrane protein-1.

* Corresponding authors.

E-mail addresses: mustafa.ghanim@najah.edu (M. Ghanim), j.amer@najah.edu (J. Amer).

¹ Authors contributed equally.

<https://doi.org/10.1016/j.bioph.2022.112942>

Received 20 February 2022; Received in revised form 26 March 2022; Accepted 6 April 2022

Available online 13 April 2022

0753-3322/© 2022 The Authors. Published by Elsevier Masson SAS. This is an open access article under the CC BY license (<http://creativecommons.org/licenses/by/4.0/>).

disease, liver cirrhosis, and cancer [9,10]. Many studies have shown EE possesses antioxidant and anti-inflammatory properties [11]. In the current study we investigated antifibrotic, antioxidant, metabolic, and immune effects of EE in an animal mice model of liver fibrosis established through thioacetamide (TAA) inductions. Moreover, we aimed to evaluate EE as a natural medication for possible mechanism in modulating disease progression.

2. Materials and methods

2.1. Drugs and chemicals

Thioacetamide (TAA, Sigma Aldrich, CAT# 172502), Sirius red F3B in saturated picric acid stain (Abcam, ab150681), H&E Staining Kit (Hematoxylin and Eosin) (Abcam, ab245880), Trichrome Stain Kit (Connective Tissue Stain) (Abcam, ab150686), TaqMan Fast Advanced Master Mix (Applied Biosystem; Cat# 4371130), Reduced glutathione (GSH) assay kit (Fluorometric, ab235670), Glutathione peroxidase assay kit (Cayman Chemicals, #703102), Catalase activity assay kit (Fluorometric, ab83464). EZ-PCR test kit (Biological Industries, 20-700-20). Ethanol (CAS 64-17-5, 100983 - Merck Millipore).

2.2. Animal model

Twelve weeks old male C57BL6/J mice received care according to the Hebrew University ethical regulations and NIH guidelines. The institutional animal care ethical committee approved all animal protocols (MD-16-14574-3). Mice, housed in a barrier facility, were intraperitoneally (i.p.) injected with thioacetamide (TAA, 200 mg/kg body weight) or PBS twice a week for four weeks. 100 mg/kg EE was injected intraperitoneally (i.p.) twice a week, starting at week 2 following TAA injections. All experiments were performed during the day. Each group included ten mice. Following 2 days of the last TAA injections, on the day they were sacrificed, mice were weighed and anesthetized intramuscularly with 0.1 ml of ketamine (20 mg/kg): xylazine (2 mg/kg): acepromazine (0.5 mg/kg) prior to cervical dislocation [12].

2.3. Preparation of the plant extract

Since July 2021, the EE's fresh mature fruits have been collected on uncultivated land in the Tulkarem governorate of Palestine (Latitude: 32°18'42"N; Longitude: 35°01'38"E). Dr. Nidal Jaradat, an expert in medicinal botanicals, recognized the EE plant in the Herbal Products Laboratory at An-Najah National University, and the sample was deposited under the voucher specimen of Pharm-PCT-870. This procedure was also in line with the WHO's Guidelines for the Evaluation of Herbal Medicines and Law Enforcement.

The collected EE mature fruits were washed with sterile water, ground, and compressed using a mechanical Juicer Extractor (Aicok Juicer, China). Plant juice was sterilized utilizing a Millipore Sigma membrane filtration device (Germany). The produced liquid was dried using a laboratory vacuum freeze dryer (TEFIC, TF-10C, Shaanxi, China) and kept in air-tight brown jars at 4°C until use.

2.4. Histological assessment

The posterior third of the lung and liver tissues were fixed in 4% formalin for 24 h and then paraffin-embedded in an automated tissue processor. Section (7 mm) were stained with H&E for evaluating steatosis, necro-inflammatory regions, and apoptotic bodies and with 0.1% Sirius red F3B in saturated picric acid stain and Masson Trichrome Stain (MTC) to visualize connective tissue. A veterinary pathologist assessed

all histopathological findings based on published parameters [13–15].

2.5. Liver and serum metabolic profile assessments

Mice whole blood samples were collected at the sacrificing day and centrifuged at 3500 rpm for 20 min at 4 °C. Serum ALT, AST, and ALP concentrations were determined. Blood sugar, cholesterol, triglycerides, and C-peptide were assessed following fasting for sixteen hours. All tests were performed at the Central lab of Hadassah Hospital, Jerusalem.

2.6. RNA isolation, cDNA preparation, and real-time PCR

Total cellular RNA was isolated from lung and liver tissue as previously described [16]. Real-time PCR was performed with TaqMan Fast Advanced Master Mix to quantify α SMA and collagen III. Gene expression was normalized to the expression of the housekeeping GAPDH gene.

2.7. Liver antioxidant activity assays

The homogenized liver tissue was centrifuged at 9000g for 15 min. The separated supernatant was used for oxidative stress assessment. Glutathione (GSH) content in liver tissue was measured with the reduced glutathione (GSH) assay kit. Glutathione peroxidase (GPX) and catalase (CAT) were measured to determine antioxidant defense enzyme activities. Glutathione peroxidase activity ($GP \times 1$) was determined using the glutathione peroxidase assay kit. The catalase activity assay kit was used according to the manufacturer's instructions.

2.8. Liver tissue-resident NK (trNK) cells isolation

Livers were removed and transferred to Petri dishes containing 10 ml DMEM medium (Biological industries; Cat# 01-055-1A). The liver tissue was thoroughly dispersed with a stainless steel mesh, and the cells were harvested with the medium and transferred to 50 ml tubes containing 10 ml DMEM. The cells were then carefully transferred to new tubes containing Ficoll (Abcam; Cat# AB18115269) and centrifuged for 20 min, at 1600 rpm at 20 °C. The supernatant of each tube was transferred to a new tube and centrifuged for 10 min at 1600 rpm at 4 °C. After the second centrifugation, the pellet in each tube was suspended in 1 ml of DMEM for NK cell isolation and purification (StemCells kit; Cat# 19665).

2.9. Primary HSCs isolation and co-culture with liver trNK cells

Primary HSCs (pHSCs) were isolated from 12-weeks-old male C57BL6/J mice by in situ pronase/ collagenase perfusion and a single-step Histogenz gradient. pHSCs (10^6 cells), were cultured in DMEM supplemented with 10% fetal calf serum, 100 units/ml penicillin and 100 mg/ml streptomycin. Cells were grown under 5% CO₂ at 37 °C and confirmed negative for mycoplasma contamination with an EZ-PCR test kit. For the co-culture experiments, pHSCs cells were cultured with trNK cells (10^6 cells) obtained from the TAA mice model treated with or without EE. All cells were incubated for 48 h.

2.10. Flow cytometry

Harvested mice liver trNK cells were adjusted to 10^6 /ml in buffer saline containing 1% bovine albumin (Biological Industries; Cat# 02-023-5A) and were stained with the following antibodies: Anti-mouse NK1.1 (murine NK cell marker) (Biogems; Cat# 83712-70), anti CD49a (MACS; Lot# 5150716246), anti CD49b (MACS; Lot# 5150716256), anti-IFN- γ and anti-mouse lysosomal-associated

membrane protein-1 (CD107a; NK1.1 cells cytotoxicity marker, eBioscience, Cat# 48-1071). All antibodies were incubated for 40 min at 4 °C. pHSCs (10^6 cells/ml) were stained with rabbit anti-mice α SMA (R&D; IC1420P). The cells were washed with 0.5 ml staining buffer and fixed with 20 ml 2% paraformaldehyde. All stained cells were analyzed with a flow cytometer (BD LSR Fortessa™, Becton Dickinson, Immunofluorescence systems, Mountain View, CA).

2.11. Immunofluorescence staining

For deparaffinization, paraffin-embedded sections were placed in a 60 °C bath for 15 min, incubated in xylene at room temperature for 15 min, and then transferred sequentially to 100%, 95%, 70%, and 50% EtOH for 4 min each at room temperature. Sections were rinsed in deionized water and stored in PBS. For antigen retrieval and anti- α SMA detection, we used a buffer (10 mM citrate, pH 6.2, 2 mM EDTA, and 0.05% Tween 20). pHSCs cell samples were treated with 100 μ L of KASBLOCK liquid blocker to minimize the volume of antibody solution needed for staining. Samples were incubated overnight at 4 °C with rabbit anti-human /mouse/rat α SMA (diluted 1:170, IQ Products, Groningen, Netherlands). Samples were washed with PBS, secondary antibodies conjugated with Cy-2 were then applied for one hour at room temperature, and image capture was performed. Samples were viewed and imaged with a Zeiss LSM 710 confocal laser scanning system (Zeiss, Germany) attached to a Zeiss Axiovert 135 M microscope, equipped with a Plan-Apochromat Zeiss 63X lens. An argon laser (488 nm excitation) was used to detect green fluorescence.

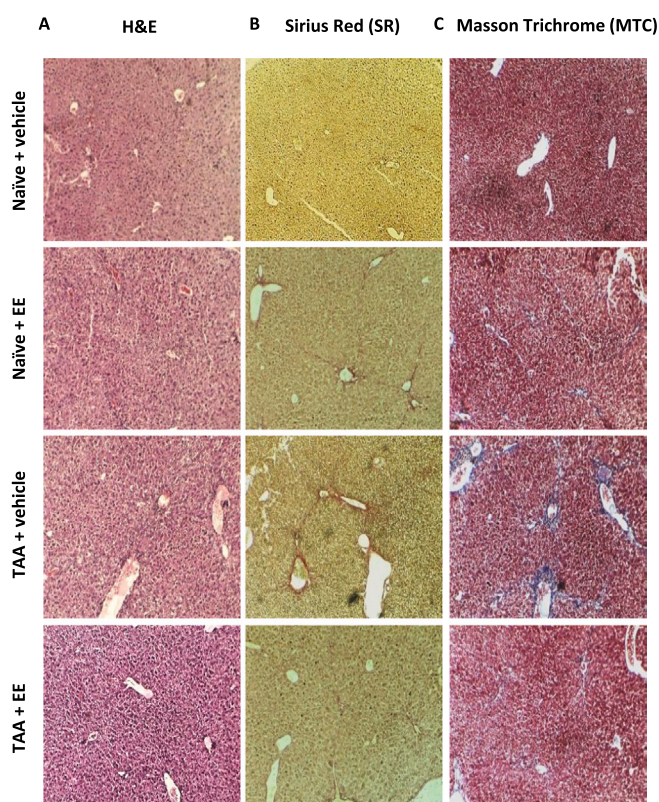
2.12. Statistical analysis

Statistical significance was determined by two-tailed unpaired Student's t-test (for comparison between two groups) and chi-square or one-way analysis of variance (one-way ANOVA with Newman-Keuls post-tests) for multiple groups with GraphPad Prism 5.0 (GraphPad Software, La Jolla, CA). In vitro experiments were repeated three times, with four sample replicates each. Data are represented as mean \pm SEM.

3. Results

3.1. Characterization of inflammatory and fibrotic profiles in TAA mice treated with *Ecballium elaterium* (EE)

Livers were assessed for liver injury and phenotypic alterations in the TAA mice following treatments with EE. Representative H&E, Sirius Red, and Masson's trichrome staining of liver sections are presented in Fig. 1A. H&E staining of TAA livers showed swelled centrilobular hepatocytes and large necrotic areas of high infiltrating inflammatory cells with steatosis. EE-treated mice showed a delay in the histological findings, with a significant reduction in micro- and macrovascular steatosis. Sirius red staining of livers from the TAA mice demonstrated increased collagen deposition in perisinusoidal areas; whereas treatment with EE resulted in a remarkable reduction in the dense fibrous tissue of the stained area. Moreover, livers following EE treatments showed minimal accumulation of thick fibrotic tissue in the TAA mice using MTC staining compared to the vehicle-treated mice. Fig. 1D summarizes a detailed histology scoring system for H&E and fibrosis assessments [12–15]. Biochemical markers were also assessed in our mice groups. Serum inflammatory profiles of ALT (Fig. 1E), AST (Fig. 1F), and ALP (Fig. 1G)



D	Naïve	Naïve+EE	TAA*	TAA+EE*	*p value
Steatosis	0	0	2 \pm 0.01	0.6 \pm 0.1	0.01
Microvesicular steatosis	0	0	1 \pm 0.5	0	0.04
Lobular Inflammation	1 \pm 0.2	0.45 \pm 0.2	3 \pm 0.1	0.5 \pm 0.2	0.015
Micro-granulomas	0	0	1 \pm 0.1	0	0.015
Portal inflammation	0	0	1 \pm 0.1	0	0.03
Ballooning	1.5 \pm 0.01	0.5 \pm 0.2	0.75 \pm 0.02	0.5 \pm 0.2	0.04
Acidophil bodies	0	0	0.5 \pm 0.3	0	0.022
Fibrosis stage (SR)	0	0	3 \pm 0.09	1 \pm 0.01	0.02
Fibrosis area % (SR)	0.2 \pm 0.01	0.26 \pm 0.02	5.1 \pm 1	1.5 \pm 0.3	0.004
Fibrosis area % (MTC)	0.15 \pm 0.01	0.14 \pm 0.01	5.7 \pm 1.4	1.3 \pm 0.5	

Steatosis: 0=<5%; 1=5-33%; 2>33-66%; 3>66%. Microvesicular steatosis: 0=Present;1=not present. Lobular Inflammation:0=no foci;1=<2 foci; 2=2-4 foci; 3=>4 foci/200x field. Micro-granulomas: 0=absent; 1=present. Portal inflammation: 0=none to minimal; 1=> than minimal. Ballooning: 0=none; 1=few; 2=many. Acidophil bodies: 0=none; 1=many. Fibrosis stages =0=none; 1=perisinusoidal or periportal;2= perisinusoidal and periportal; 3=bridging fibrosis; 4= Cirrhosis.

Fig. 1. The inflammatory and fibrotic profile. Liver fibrosis was induced in C57/BL mice for 4 weeks and was compared to naïve counterparts (10 mice per group; each experiment was repeated three times). EE was injected i.p. for 2 weeks, starting at week 2 of TAA, as described in the Materials and Methods section. Representative sections of immunohistochemical liver staining of (A) H&E, (B) Sirius red, and (C) Masson's trichrome (original magnification 10x). (D) Quantification of liver histology assessments are summarized and represented as average \pm SEM (10 mice per group). Liver injury markers of serum are (E) ALT, (F) AST, (G) ALP. Liver fibrosis mRNA markers of (H) α SMA and (I) collagen III were assessed. Each experiment was repeated three times.

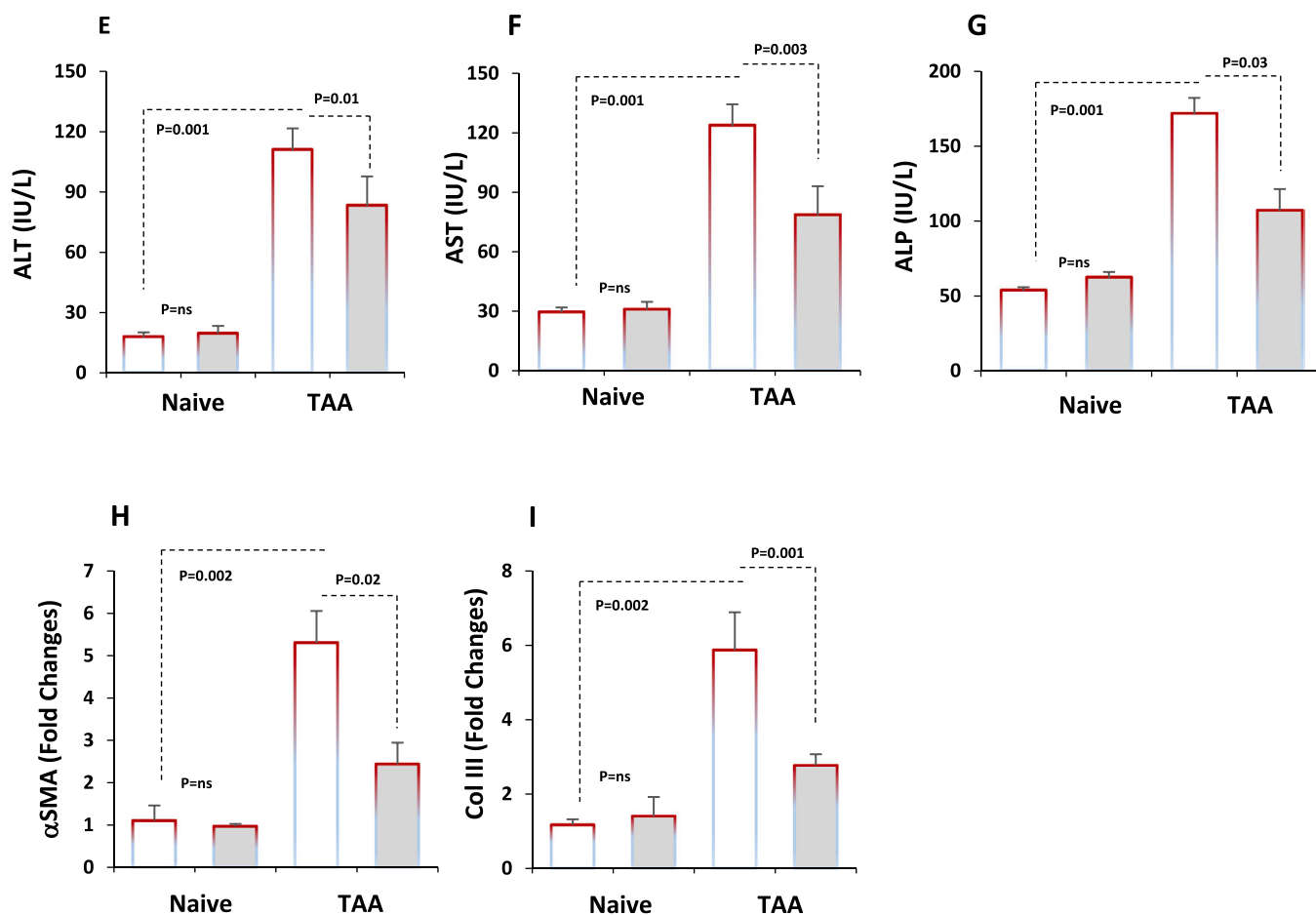


Fig. 1. (continued).

showed a significant amelioration of 1.32-fold, 1.57-fold, and 1.6-fold, respectively ($P < 0.05$), following treatment with EE in the TAA mice. Fibrosis marker quantitation was made for the TAA induced mice to confirm liver fibrosis through assessing liver α SMA and collagen III (Col III) by RT-PCR. Data showed a significant increase in α SMA and Col III (4.8-fold and 5.2-fold, respectively; $p = 0.002$) compared to mice receiving the vehicle (Figs. 1H and 1I). Liver fibrosis mice receiving EE treatments demonstrated significant reductions in α SMA and Col III by 2.2-fold and 2.1-fold, respectively ($P < 0.03$). Comparable results were achieved between the RT-PCR and histology assessments and clearly indicate (1) amelioration of liver fibrosis and (2) improved liver histology of inflammation and fibrosis in liver sections following treatments with EE.

3.2. Metabolic and oxidative stress assessments in the TAA-induced liver damage mice model

TAA potentiates high cholesterol and high-fat diet-induced steatohepatitis changes in the livers of C57BL/6J mice [17]. Moreover, TAA showed an increased hepatic lipid profile of cholesterol, fatty acids, and triglycerides in chronic and acute treatment in rats [18]. Therefore, we adopted this model to characterize metabolic outcome markers of lipid and glucose profiles following treatments with EE. Our mice model showed metabolic profile perturbation in the TAA-induced animals. Fig. 2 displays an increase in serum levels of cholesterol (Fig. 2A), triglyceride (Fig. 2B), C-peptide (insulin) (Fig. 2C), and FBS (Fig. 2D) in the

TAA mice. These mice treated with EE maintained low serum levels of cholesterol, triglycerides, and C-peptide compared to naïve groups receiving the vehicle while showed a reduction in their FBS (Fig. 2D). Altogether, the above data indicate that EE has an antifibrotic effect, most probable due to their effects in ameliorating lipid and glucose profiles, both of which are risk factors contributing to fibrogenesis. Thus, our results indicate EE as a potential target for delaying and inhibiting liver fibrosis through improving insulin sensitivity. To further explore the mechanism behind the antifibrotic effects of EE, their antioxidant properties were evaluated. TAA itself is not hepatotoxic, and its active metabolites covalently bind to proteins and lipids, causing oxidative stress leading to central lobular necrosis of the liver [19]. Fig. 3 shows assessments of liver antioxidant enzymes of reduced glutathione (GSH), glutathione peroxidase (GPX), and catalase. Liver fibrosis mice of TAA-induced and treated with EE exhibited a significant increase of 1.4-fold, 2-fold, and 1.31-fold of GSH (Fig. 3A), GPX (Fig. 3B), and CAT (Fig. 3C), respectively. Our generated data were consistent with another report [20] showing that the progress of a liver injury is closely related to the downregulation of antioxidant enzymes in the liver. In our study, EE enhanced the activity of these enzymes and the liver function, counteracting hepatotoxicity.

3.3. *Ecballium elaterium* (EE) has an anti-inflammatory effect due to the reduction of inflammatory cytokines

A panel of inflammatory cytokines representing various

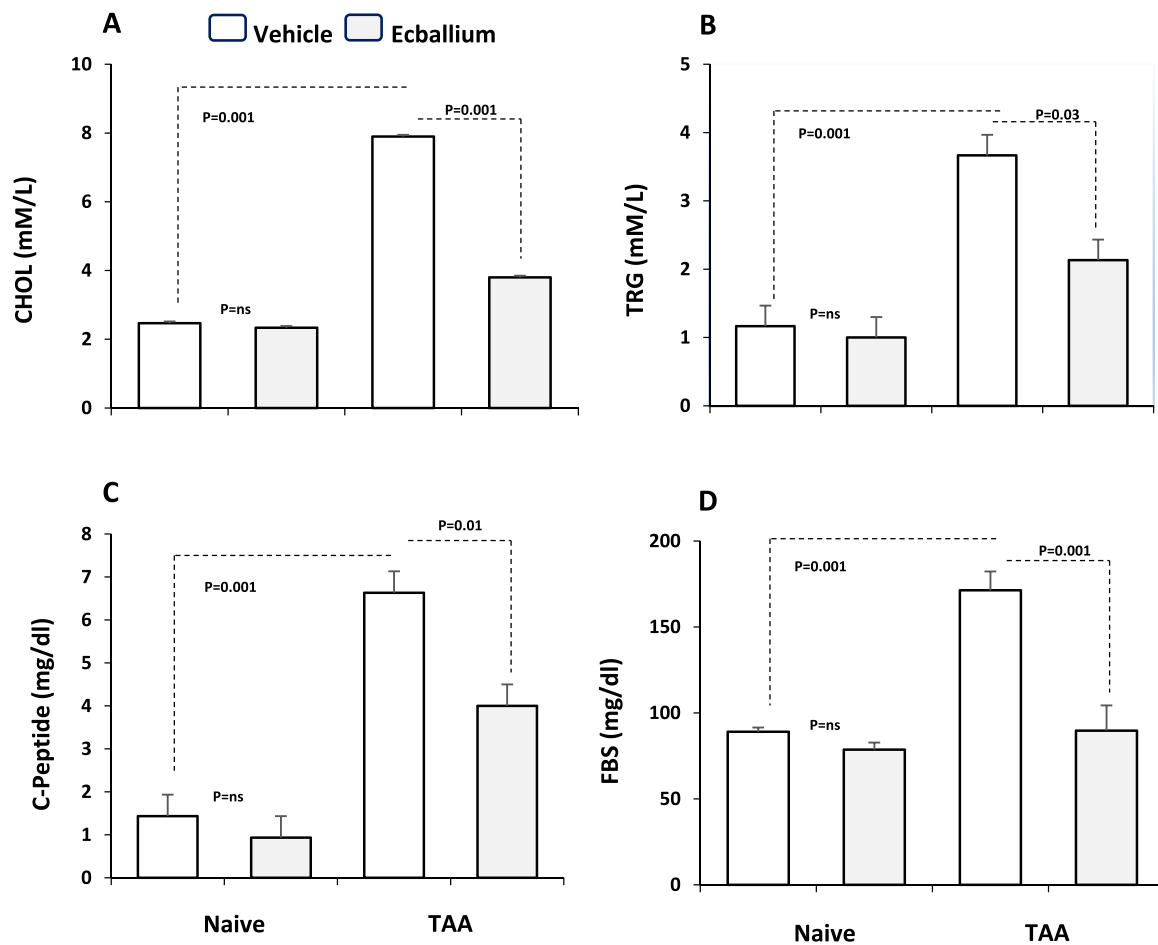


Fig. 2. EE improved the perturbed metabolic profile in TAA-induced animals. Metabolic markers of lipid and glucose profile of serum levels of (A) cholesterol, CHOL, (B) triglyceride, TRG, (C) C-peptide, and (D) fasting blood sugar (FBS) were assessed following sixteen hours of fasting. Each measurement was repeated three times and data represented as mean \pm SEM.

inflammatory pathways were assessed. Cytokines are significant mediators in the pathophysiology of liver fibrosis [21]. Thus, we measured serum cytokines to investigate the possible mechanisms by which EE could exhibit hepatoprotective effects. Fig. 4 shows the TAA mice treated with EE resulted in suppressive effects on IL-20 (Fig. 4A), TGF β (Fig. 4B), IL-17 (Fig. 4C), IL-22 (Fig. 4D) and MCP-1 (Fig. 4E) while increased the levels of the anti-inflammatory cytokine IL-15 (Fig. 4F; $p = 0.03$). The results are further supported by other studies showing that EE might play a protective role in sepsis prevention and treatment by decreasing IL-6 production and reducing liver damage and may influence bacterial translocation by reinforcing intestinal barrier function [22]. Moreover, our data suggest that effects of EE in improving liver injury profile and modulating cytokines concentrations could highlight the involvement of immune cells as a crucial element in liver fibrogenesis.

3.4. EE treated TAA-mice showed liver recruitment of trNK cells and restored their activity

The immune system plays a central role in tissue healing. Therefore, control of the immune system is critical in planning the healing process [23]. Larouche et al. [24] showed increased neutrophil leukocyte numbers and decreased fibrosis in the skin following EE extract treatment. However, these studies did not describe the mechanism behind

the hepatoprotective effect. We evaluated the isolated liver tissue-resident NK cells (trNK) extracted from our mice groups. NK cells showed no exert an antifibrotic effect by killing activated HSCs [25]. Fig. 5A shows an elevated trNK percentages in the TAA-induced mice following treatments with EE extracts (5-fold; $p = 0.001$). Moreover, trNK intracellular expressions of CD107a (Fig. 5B) and INF- γ (Fig. 5C) showed an 6 and 13.5 fold increase following the EE treatments as compared to controls, respectively ($p < 0.01$). To further associate trNK stimulatory effects with their cytotoxicity potentials, we co-incubated isolated trNK cells with activated liver primary HSCs [26] obtained from TAA-induced mice. Fig. 5D shows a significant reduction of 16-fold in α SMA intensities in primary HSCs following their co-culture with EE-treated trNK obtained from the TAA-induced mice as compared to mice receiving the vehicle ($p = 0.0001$). The above results were confirmed by confocal microscopy, showing reduced α SMA immunofluorescence by activated primary HSCs (Fig. 5E). Our results undoubtedly indicate the impact of EE as a potential therapy as they exhibit antifibrotic and antioxidative effects by reducing α SMA and reactive oxygen species (ROS) by activated HSCs, respectively and could be of beneficial influence for patients with advanced liver injury.

4. Discussion

The current study evaluated the potential ameliorating effect of EE

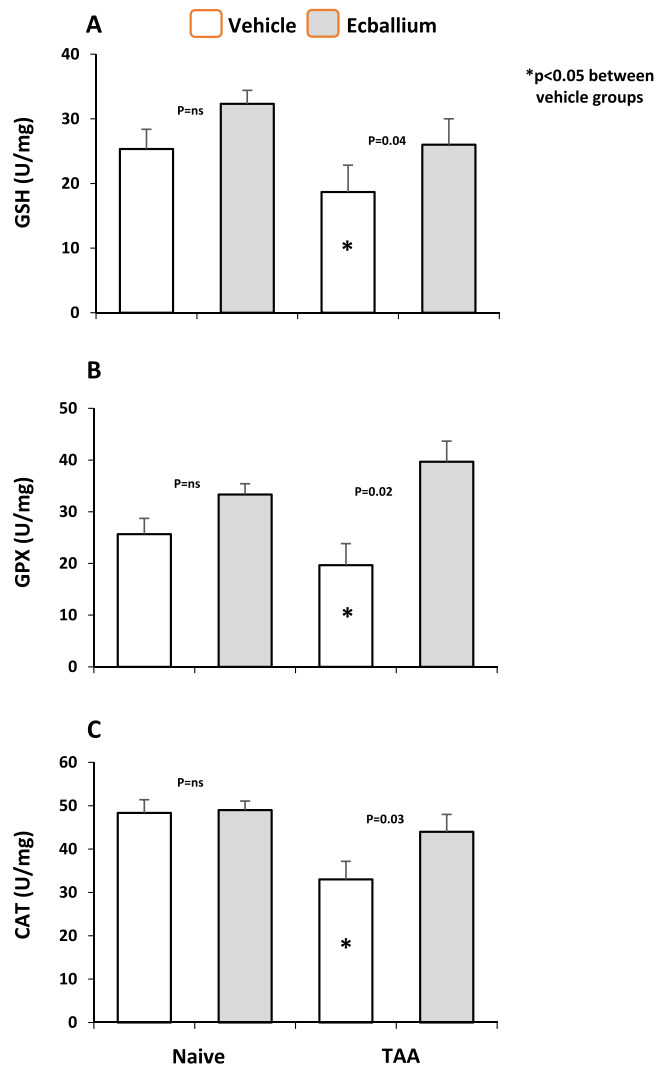


Fig. 3. EE exhibits liver antioxidant activity. Liver concentrations of (A) glutathione (GSH), (B) glutathione peroxidase (GPX), and (C) catalase (CAT) were assessed by ELISA.

on hepatic histopathological, immunological, and biochemical alterations in the TAA-mice model. EE is a Mediterranean plant used in traditional medicine. Its fruits and fruit juice are mainly administered for several therapeutic uses, although they can be toxic at high doses [27]. Some studies have described its cytotoxic effects against cancer cells and its neuroprotective and hepatoprotective roles [22,28,29]. Our current study used a liver injury mice model established by treating mice with TAA. This model features a metabolic profile of excessive fatty acid oxidation, insufficient glutathione regeneration, and disturbed gut flora. Further characteristics include an inhibited urea cycle, DNA damage, a perturbed Krebs cycle, and branched-chain amino acid oxidation in the bile duct ligation [30]. In terms of clinical features, TAA-induced hepatic inflammation, fibrosis, and liver damage in mice are very close to chronic human liver disease [31]. After TAA exposure, liver injury is propagated due to hepatocyte membrane damage, which causes leakage of transaminase enzymes into the circulation [32]. The liver toxicity results from TAA bioactivation led by a mixed-function oxidase system, including the cytochrome P2E1 and flavin adenine dinucleotide monooxygenases [33]. Furthermore, the activation of TAA causes the formation of reactive metabolites such as thioacetamide-S-oxide radicals

and (ROS) intermediates [34].

There is scant data on the hepatoprotective effect of EE. Agil et al. [35] focused on the hepatoprotective effect of EE and cucurbitacin B isolated from the juice. Their study employed a model of CCl₄-induced hepatotoxicity and showed prophylactic and therapeutic administration of these substances [28]. In addition, Uslu et al. showed that EE exerted an anti-inflammatory effect by inhibiting nitric oxide synthase [36]. The overproduction of hepatic ROS was predominantly accelerated in inflammatory liver injuries, affecting the hepatic structure and leading to severe hepatocellular dysfunction with a poor prognosis [37,38].

Our present study found a significant antioxidant effect of EE in the TAA-induced mice model (Fig. 3). Therefore, EE treatment could be a potential antifibrotic strategy targeting HSCs activation by lowering the impact of free radicals, known as a feature of chronic liver disease. Oxidative stress plays a role in HSCs activation [39], and ROS produced by damaged hepatocytes provide paracrine activation signals to HSCs [40]. Moreover, ROS and lipid peroxidation products also stimulate the synthesis of extracellular matrix (ECM) by activated HSCs [41]. Elayan et al. [42] showed that the administration of EE juice to rats decreased bilirubin levels, without identifying the mechanism. The modification of the bilirubin levels in the plasma may arise from the effect of the juice on the liver function, particularly the glucurono conjugation, or by modifying the bilirubin binding to albumin in plasma [43]. Here, we report additional effects of EE on the metabolic profile associated with advanced liver fibrosis. Lipids and glucose are major risks in the pathogenesis of liver injury and are associated with morbidity due to diabetes and atherosclerosis. Free cholesterol activates HSCs, and the addition of cholesterol to a high-fat or methionine/choline-deficient diet leads to the accumulation of free cholesterol in HSCs, which accelerates experimental liver fibrosis [44]. High hepatocyte lipid droplet accumulation in the livers propagates liver injury and causes a storm of pro-inflammatory cytokines that can lead to steatosis and hepatocyte injury [45]. Fig. 2 displays alleviation in metabolic markers of cholesterol, triglycerides, C-peptide, and fasting blood sugar following EE treatment. The data may indicate improved liver histology; thus, minimizing the progression of liver fibrosis could be partly achieved by targeting the metabolic profile. Moreover, in our study we assessed EE effects of selected pro- and anti-inflammatory cytokines and their interference with liver fibrosis progression or resolution. For instance, IL-15 and IL-15 receptor α have a protective role in liver fibrosis progression by regulating fibrogenic molecules and collagen expression in HSCs and maintaining NK cell homeostasis [46]. In contrast, IL-20 is a pro-inflammatory cytokine of the IL-10 family that activates quiescent HSCs and upregulates TGF β expression. In mice, administration of antibodies neutralizing either IL-20 or the IL-20 receptor inhibits CCl₄-induced cell damage, TGF β production, HSCs activation, and liver fibrosis [47]. On the other hand, IL-17 induced the production of type I collagen in HSCs by activating the signal transducer and activator of transcription 3 (STAT3) signaling pathway [48]. Furthermore, IL-22 showed an important role for the modulation of tissue responses during inflammation. Through activation of Stat3-signaling cascades, IL-22 induces proliferative and anti-apoptotic pathways [49]. MCP-1 on the other hand, is a chemokine that regulates migration and infiltration of monocytes/macrophages. MCP-1 showed to regulate CD56⁺ NK cells, which consequently inhibits perforin expression and results in a decrease of NK cells cytotoxicity [50]. Our data revealed that EE exhibits anti-inflammatory effects by modulating secreted cytokines through the increase in IL15 and decrease in IL-20, IL-17, IL-22, and TGF β . These results are in agreement with previous evidence indicating that free cholesterol accumulation in HSCs sensitizes the cells to TGF β -induced activation through enhancement of Toll-like receptor 4 (TLR4)-mediated downregulation of the TGF β pseudoreceptor BAMBI (bone

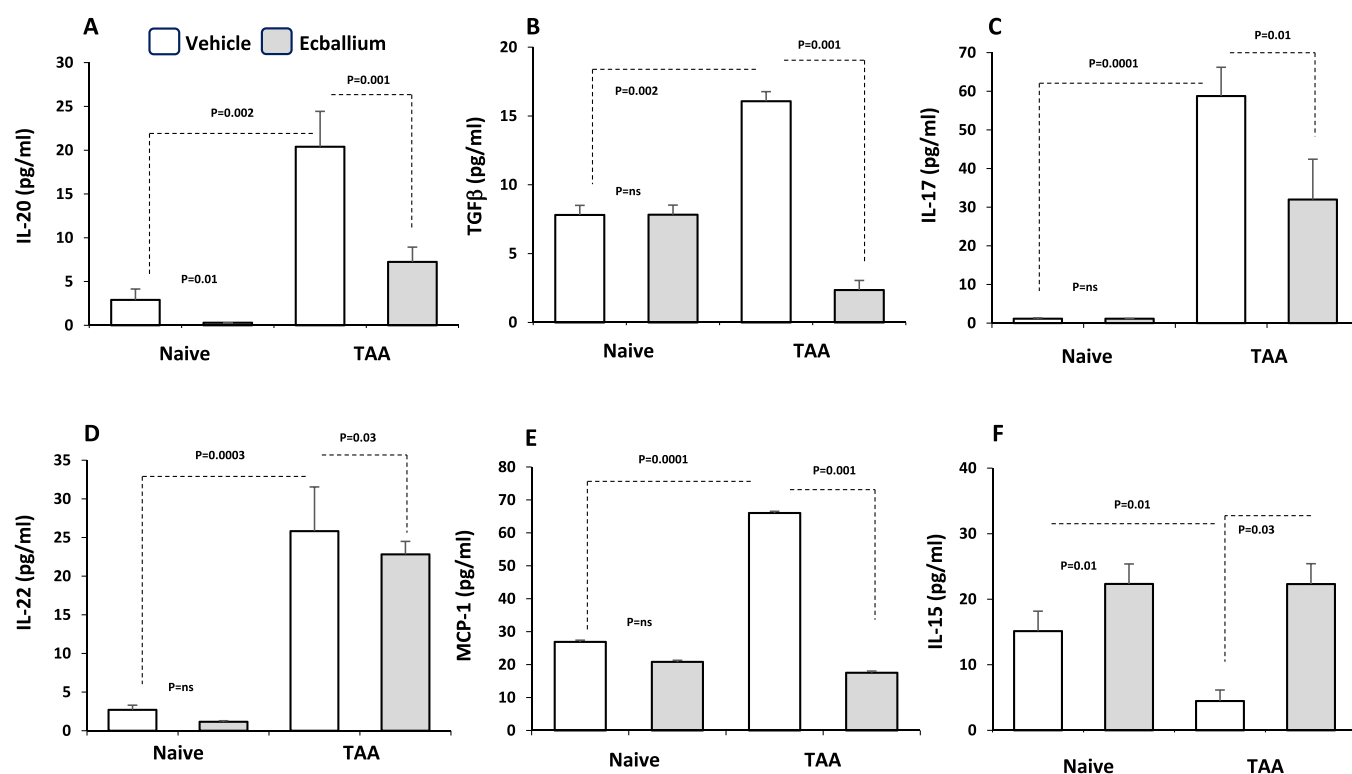


Fig. 4. EE displays an anti-inflammatory effect by reducing inflammatory cytokines. Pro-inflammatory cytokine levels of (A) IL-20, (B) TGFβ, (C) IL-17, (D) IL-22, (E) MCP-1, and (F) IL-15 were measured in all groups in triplicates. Data were analyzed using a Quantibody Q-Analyzer and an Excel-based program; results are presented in pg/ml. Data show mean ± SEM.

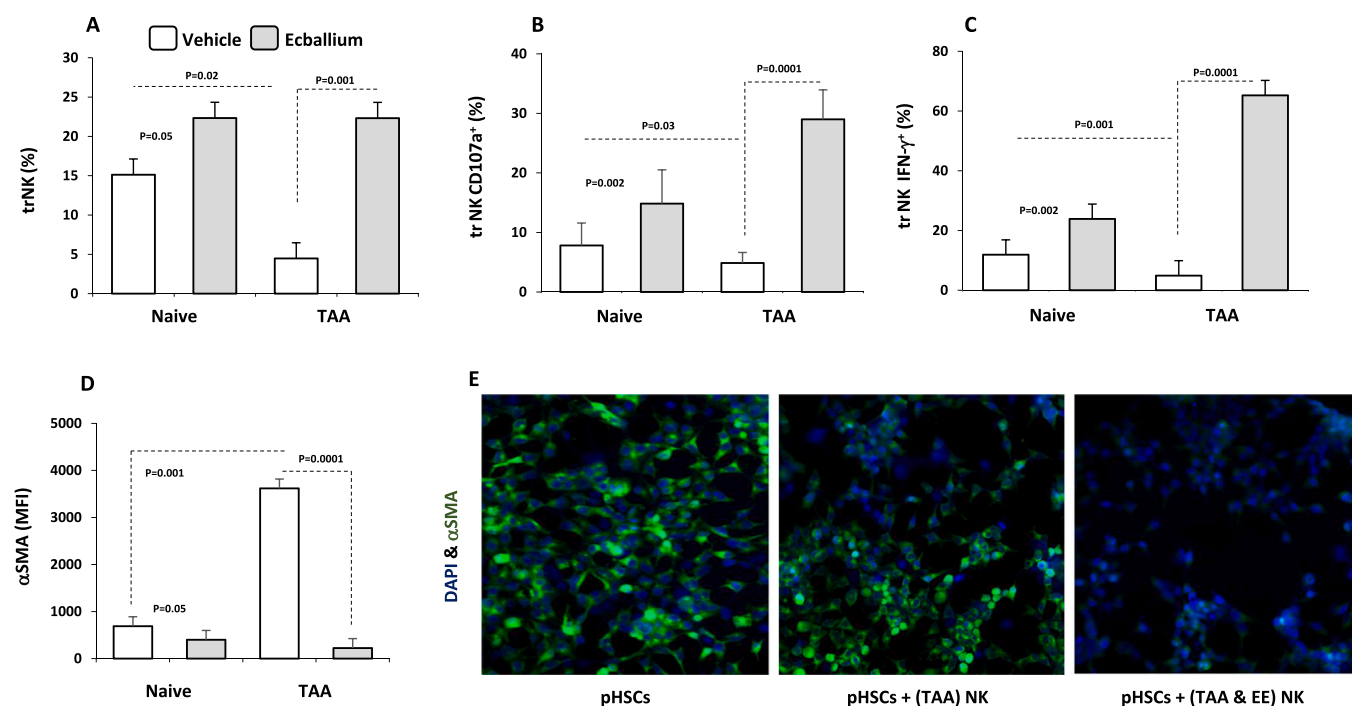


Fig. 5. EE ameliorates liver fibrosis by improving liver trNK cytotoxic effects. (A) Liver flow cytometry analysis showed high counts of trNK 1.1/CD49a⁺/CD49b⁻ cells following treatment in the vehicle and Ecballium groups. (B-C) Liver trNK 1.1/CD49a⁺/CD49b⁻ showed increased levels of (B) CD107a and (C) IFN-γ in mice in the EE-treated group (p = 0.0001). (D) trNK-EE treatment caused diminished pHSCs αSMA intensity following co-culture in the TAA treated mice. (E) Representative confocal microscopy images show diminished green staining of pHSCs following co-culture of trNK cells treated with EE in the TAA mice model. Each experiment was repeated three times and data represented as mean ± SEM.

morphogenetic protein and activin membrane-bound inhibitor) [51]. Hepatic insulin resistance is characterized by an impaired ability of insulin to decrease net glucose output from the liver, which contributes to increased blood glucose [52]. EE regulates glucose and lipid metabolism and can negatively modulate HSCs activation and fibrosis progression. Supporting data (Fig. 5) shows an increase in α SK cells in the liver following EE treatment in the TAA model associated with decreased cytotoxicity and the potential to reduce the activation of HSCs. This finding may partly explain EE's role in delaying liver fibrosis progression by minimizing α SMA and ROS productions from activated HSCs.

Overall, this study offers an overview of the biological impact of EE on liver fibrosis in a TAA-induced animal model. Its therapeutic value warrants further investigation.

CRedit authorship contribution statement

Mustafa Ghanim: Conceptualization, Project administration. **Johnny Amer:** Writing - Review & Editing, Conceptualization, Supervision, Data Curation, Project administration, Funding acquisition, Writing - Original Draft, Formal analysis. **Ahmad Salhab:** Investigation, Resources, Validation, Formal analysis. **Nidal Jaradat:** Methodology, Conceptualization, Software, Writing - Review & Editing.

Conflict of interest statement

The authors declare that they have no conflict of interest.

Data availability

Data will be made available on request.

References

- J.K. Jose, R. Kuttan, Hepatoprotective activity of emblica officinalis and chyavanaprash, *J. Ethnopharmacol.* 72 (1–2) (2000) 135–140.
- Q. Chen, H. Zhang, Y. Cao, et al., Schisandrin B attenuates CCl₄-induced liver fibrosis in rats by regulation of Nrf2-ARE and TGF- β /Smad signaling pathways, *Drug Des. Dev. Ther.* 11 (2017) 2179–2191.
- M.-J. Shi, X.-L. Yan, B.-S. Dong, W.-N. Yang, S.-B. Su, H. Zhang, A network pharmacology approach to investigating the mechanism of Tanshinone IIA for the treatment of liver fibrosis, *J. Ethnopharmacol.* 253 (2020), 112689.
- K. Damiris, Z.H. Tafesh, N.P. Tafesh, N. Pyrsopoulos, Efficacy and safety of anti-hepatic fibrosis drugs, *World Gastroenterol.* 26 (41) (2020) 6304–6321.
- E. Mormone, J. George, Molecular pathogenesis and current treatment of liver fibrosis, *Chem. -Biol. Interact.* 193 (2011) 225–231.
- P. Marcellin, E. Gane, M. Buti, et al., Regression of cirrhosis during treatment with tenofovir disoproxil fumarate for chronic hepatitis B: a 5-year open-label follow-up study, *DeLancet* 381 (2013) 468–475.
- T. Wang, W. Jin, Q. Huang, et al., Clinical efficacy and safety of eight traditional Chinese medicine combined with entecavir in the treatment of chronic hepatitis B liver fibrosis in adults: a network meta-analysis, *Evid.-based Complement. Altern. Med.* 2020 (2020), 7603410, 15 pages.
- S. Rius-Pérez, S. Pérez, P. Martí-Andrés, M. Monsalve, J. Sastre, Nuclear factor kappa b signaling complexes in acute inflammation, *Antioxid. Redox Signal.* 33 (3) (2020) 145–165.
- E. Sezik, E. Yeşilada, M. Tabata, et al., Traditional medicine in Turkey VIII. Folk medicine in east anatolia; Erzurum, Erzinçan, Ağrı, Kars, Iğdır provinces, *Econ. Bot.* 51 (3) (1997) 195–211.
- E. Yeşilada, O. Ustün, E. Sezik, et al., Inhibitory effects of Turkish folk remedies on inflammatory cytokines: Interleukin-1 α , interleukin-1 β and tumor necrosis factor α , *J. Ethnopharmacol.* 58 (1) (1997) 59–73.
- L. Bourebaba, B. Gilbert-López, N. Oukil, et al., Phytochemical composition of *Ecballium elaterium* extracts with antioxidant and anti-inflammatory activities: comparison among leaves, flowers and fruits extracts, *Arab J. Chem.* 13 (1) (2020) 3286–3300.
- M.C. Wallace, K. Hamesch, M. Lunova, Y. Kim, R. Weiskirchen, P. Strnad, S. L. Friedman, Standard operating procedures in experimental liver research: thioacetamide model in mice and rats, *Lab. Anim.* 49 (1 Suppl) (2015) 21–29.
- P.J. Scheuer, Classification of chronic viral hepatitis: a need for reassessment, *J. Hepatol.* 13 (1991) 372–374.
- P. Bedossa, T. Poynard, An algorithm for grading activity in chronic hepatitis C, *Hepatology* 24 (1996) 289–293.
- K. Ishak, A. Baptista, L. Bianchi, F. Callea, J. De Groote, F. Gudat, H. Denk, V. Desmet, G. Korb, R.N. MacSween, Histological grading and staging of chronic hepatitis, *J. Hepatol.* 22 (1995) 696–699.
- A. Salhab, J. Amer, Y. Lu, R. Safadi, Sodium+/taurocholate cotransporting polypeptide as target therapy for liver fibrosis, *Gut* (2021). Jul 15;gutjnl-2020-323345.
- L. Sharma, D. Gupta, S.T. Abdullah, Thioacetamide potentiates high cholesterol and high fat diet induced steato-hepatic changes in livers of C57BL/6J mice: A novel eight weeks model of fibrosing NASH, *Toxicol. Lett.* 304 (2019) 21–29.
- A.M. Bassi, P. Romano, S. Mangini, M. Colombo, C. Canepa, G. Nanni, A. Casu, Protein and m-RNA expression of farnesyl-transferases, RhoA and RhoB in rat liver hepatocytes: action of perillyl alcohol and vitamin A in vivo, *J. Biomed. Sci.* 12 (3) (2005) 457–466.
- Y.L. Bao, L. Wang, H.T. Pan, T.R. Zhang, Y.H. Chen, S.J. Xu, X.L. Mao, S.W. Li, Animal and organoid models of liver fibrosis, *Front. Physiol.* 12 (2021), 666138.
- S. Li, H.Y. Tan, N. Wang, et al., The role of oxidative stress and antioxidants in liver diseases, *Int. J. Mol. Sci.* 16 (11) (2015) 26087–26124.
- H.J. Zhangdi, S.B. Su, F. Wang, et al., Crosstalk network among multiple inflammatory mediators in liver fibrosis, *World J. Gastroenterol.* 25 (33) (2019) 4835–4849.
- M.S. Arslan, E. Basuguy, I. Ibiloglu, E. Bozdemir, H. Zeytun, A. Sahin, I. Kaplan, B. Aydogdu, S. Otcu, Effects of *Ecballium elaterium* on proinflammatory cytokines in a rat model of sepsis, *J. Invest. Surg.* 29 (6) (2016) 399–404.
- M. Cohen-Naftaly, S.L. Friedman, Current status of novel antifibrotic therapies in patients with chronic liver disease, *Ther. Adv. Gastroenterol.* 4 (6) (2011) 391–417.
- J. Larouche, S. Sheoran, K. Maruyama, et al., Immune regulation of skin wound healing: mechanisms and novel therapeutic targets, *Adv. Wound Care* 7 (7) (2018) 209–231.
- N. Muhanna, S. Doron, O. Wald, A. Horani, A. Eid, O. Pappo, S.L. Friedman, R. Safadi, Activation of hepatic stellate cells after phagocytosis of lymphocytes: a novel pathway of fibrogenesis, *Hepatology* 48 (3) (2008) 963–977.
- A. Salhab, J. Amer, L. Yinying, et al., 25(OH) D3 alleviate liver NK cytotoxicity in acute but not in chronic fibrosis model of BALB/c mice due to modulations in vitamin D receptor, *BMC Gastroenterol.* 20 (2020) 102.
- L. Bourebaba, B. Gilbert-López, N. Oukil, F. Bedjou, Phytochemical composition of *Ecballium elaterium* extracts with antioxidant and anti-inflammatory activities: Comparison among leaves, flowers and fruits extracts, *Arab. J. Chem.* 13 (2020) 3286–3300.
- M.B. El Naggari, M. Chalupova, G. Prazanova, et al., Hepatoprotective and proapoptotic effect of *Ecballium elaterium* on CCl₄-induced hepatotoxicity in rats, *Asian Pac. J. Trop. Med.* 8 (2015) 526–531.
- A.M. Arel-Dubeau, F. Longpre, J. Bournival, et al., Cucurbitacin E has neuroprotective properties and autophagic modulating activities on dopaminergic neurons, *Oxid. Med. Cell Longev.* 2014 (2014), 425496.
- Wei Dan-Dan, Wang Jun-Song, Duan Jin-Ao, Kong Ling-Yi, Metabolomic assessment of acute cholestatic injuries induced by thioacetamide and by bile duct ligation, and the protective effects of Huang-Lian-Jie-Du-Decoction, *Front. Pharmacol.* 9 (May) (2018) 1663–9812.
- M.-Y. Tsai, W.-C. Yang, C.-F. Lin, C.-M. Wang, H.-Y. Liu, C.-S. Lin, J.-W. Lin, W.-L. Lin, T.-C. Lin, P.-S. Fan, K.-H. Hung, Y.-W. Lu, G.-R. Chang, The ameliorative effects of fucoidan in thioacetamide-induced liver injury in mice, *Molecules* 26 (2021) 1937.
- M.C. van de Poll, J.P. Derikx, W.A. Buurman, et al., Liver manipulation causes hepatocyte injury and precedes systemic inflammation in patients undergoing liver resection, *World J. Surg.* 31 (10) (2007) 2033–2038.
- S.M. Salama, A.S. AlRashdi, M.A. Abdulla, P. Hassandarvish, M. Bilgen, Protective activity of Panduratin A against thioacetamide-induced oxidative damage: demonstration with in vitro experiments using WRL-68 liver cell line, *BMC Complement. Alter. Med.* 13 (2013) 279.
- J. Chilakapati, K. Shankar, M.C. Korrapati, R.A. Hill, H.M. Mahendale, Saturation toxicokinetics of thioacetamide: Role in initiation of liver injury, *Drug Metab. Dispos.* 33 (2005) 1877–1885.
- A. Agil, M. Miró, J. Jimenez, J. Aneiros, M.D. Caracul, A. García-Granados, M. C. Navarro, Isolation of anti-hepatotoxic principle form the juice of *Ecballium elaterium*, *Planta Med.* 65 (7) (1999) 673–675.
- İbiloglu İbrahim, Alabalik Ulas, Nur Keles Ayse, Aydogdu Gulay, Basuguy Erol, Buyukbayram Huseyin, *Ecballium elaterium* extract reduces fibrosis during wound healing in rats, *Biotechnol. Biotechnol. Equip.* 35 (1) (2021) 696–703.
- N. Sakai, H.L. Van Sweringen, R.M. Belizaire, R.C. Quillin, R. Schuster, J. Blanchard, J.M. Burns, A.D. Tevar, M.J. Edwards, A.B. Lentsch, Interleukin-37 reduces liver inflammatory injury via effects on hepatocytes and non-parenchymal cells, *J. Gastroenterol. Hepatol.* 27 (2012) 1609–1616.
- H. Jaeschke, Reactive oxygen and mechanisms of inflammatory liver injury: present concepts, *J. Gastroenterol. Hepatol.* 26 (Suppl. 1) (2011) 173–179.
- D. Dhar, J. Baglieri, T. Kisseleva, D.A. Brenner, Mechanisms of liver fibrosis and its role in liver cancer, *Exp. Biol. Med.* 245 (2) (2020) 96–108.
- C.R. Gandhi, Oxidative stress and hepatic stellate cells: a paradoxical relationship, *Trends Cell Mol. Biol.* 7 (2012) 1–10.
- T. Tsuchida, S.L. Friedman, Mechanisms of hepatic stellate cell activation, *Nat. Rev. Gastroenterol. Hepatol.* 14 (7) (2017) 397–411.
- H.H. Elayan, M.N. Garaibeh, S.M. Zmeili, S.A. Salhab, Effects of *Ecballium elaterium* juice on serum bilirubin concentration in male rats, *Int. J. Crude Drug Res.* 27 (1989) 227–234.
- J.D. Ostrow, P. Mukerjee, C. Tiribelli, Structure and binding of unconjugated bilirubin: relevance for physiological and pathophysiological function, *J. Lipid Res.* 35 (1994) 1715–1737.

- [44] K. Tomita, et al., Free cholesterol accumulation in hepatic stellate cells: mechanism of liver fibrosis aggravation in nonalcoholic steatohepatitis in mice, *Hepatology* 59 (2014) 154–169.
- [45] L. Chin, N.D. Theise, A.E. Loneker, P.A. Janmey, R.G. Wells, Lipid droplets disrupt mechanosensing in human hepatocytes, *Am. J. Physiol. Gastrointest. Liver Physiol.* 319 (1) (2020) G11–G22.
- [46] J. Jiao, et al., Interleukin-15 receptor alpha on hepatic stellate cells regulates hepatic fibrogenesis in mice, *J. Hepatol.* 65 (2016) 344–353.
- [47] Y.S. Chiu, C.C. Wei, Y.J. Lin, Y.H. Hsu, M.S. Chang, IL-20 and IL-20R1 antibodies protect against liver fibrosis, *Hepatology* 60 (2014) 1003–1014.
- [48] F. Meng, et al., Interleukin-17 signaling in inflammatory, Kupffer cells, and hepatic stellate cells exacerbates liver fibrosis in mice, *Gastroenterology* 143 (765–776) (2012), e3.
- [49] A. Lauren, Zenewicz, A. Flavell Richard, Recent advances in IL-22 biology, *Int. Immunol.* 23 (3) (2011) 159–163.
- [50] X. Xu, Q. Wang, B. Deng, H. Wang, Z. Dong, X. Qu, B. Kong, Monocyte chemoattractant protein-1 secreted by decidual stromal cells inhibits NK cells cytotoxicity by up-regulating expression of SOCS3, *PLoS One* 7 (7) (2012), e41869.
- [51] T. Teratani, et al., A high-cholesterol diet exacerbates liver fibrosis in mice via accumulation of free cholesterol in hepatic stellate cells, *Gastroenterology* 142 (152–164) (2012), e10.
- [52] M. Hatting, C.D.J. Tavares, K. Sharabi, A.K. Rines, P. Puigserver, Insulin regulation of gluconeogenesis, *Ann. N. Y. Acad. Sci.* 1411 (1) (2018) 21–35.